Available online at www.sciencedirect.com
ScienceDirect
Experimental Neurology 207 (2007) 186–194
Experimental Neurology
www.elsevier.com/locate/yexnr

Slit modulates cerebrovascular inflammation and mediates neuroprotection against global cerebral ischemia

Tamer Altay [a], BethAnn McLaughlin [d], Jane Y. Wu [e], T.S. Park [a,b], Jeffrey M. Gidday [a,c,*]

[a] Department of Neurosurgery, Washington University School of Medicine, St. Louis, MO 63110, USA
[b] Department of Anatomy and Neurobiology, Washington University School of Medicine, St. Louis, MO 63110, USA
[c] Department of Cell Biology and Physiology, Washington University School of Medicine, St. Louis, MO 63110, USA
[d] Department of Pediatrics, Vanderbilt University School of Medicine, Nashville, TN 37232, USA
[e] Department of Neurology and Center for Genetic Medicine, Northwestern University, Chicago, IL 60611, USA

Received 10 February 2007; revised 23 May 2007; accepted 5 June 2007
Available online 26 July 2007

Abstract

Cerebrovascular inflammation contributes to secondary brain injury following ischemia. Recent *in vitro* studies of cell migration and molecular guidance mechanisms have indicated that the Slit family of secreted proteins can exert repellant effects on leukocyte recruitment in response to chemoattractants. Utilizing intravital microscopy, we addressed the role of Slit in modulating leukocyte dynamics in the mouse cortical venular microcirculation *in vivo* following TNFα application or global cerebral ischemia. We also studied whether Slit affected neuronal survival in the mouse global ischemia model as well as in mixed neuronal–glial cultures subjected to oxygen–glucose deprivation. We found that systemically administered Slit significantly attenuated cerebral microvessel leukocyte–endothelial adherence occurring 4 h after TNFα and 24 h after global cerebral ischemia. Administration of RoboN, the soluble receptor for Slit, exacerbated the acute chemotactic response to TNFα. These findings are indicative of a tonic repellant effect of endogenous Slit in brain under acute proinflammatory conditions. Three days of continuous systemic administration of Slit following global ischemia significantly attenuated the delayed neuronal death of hippocampal CA1 pyramidal cells. Moreover, Slit abrogated neuronal death in mixed neuronal–glial cultures exposed to oxygen–glucose deprivation. The ability of Slit to reduce the recruitment of immune cells to ischemic brain and to provide cytoprotective effects suggests that this protein may serve as a novel anti-inflammatory and neuroprotective target for stroke therapy.
Published by Elsevier Inc.

Keywords: Stroke; TNFα; Leukocytes; Chemotaxis

Introduction

Cerebrovascular inflammation occurs in response to various stimuli including cytokines (Blond et al., 2002; Stanimirovic and Satoh, 2000), chemokines (Cartier et al., 2005), and ischemia (del Zoppo et al., 2000). Slit, a secreted glycoprotein previously known for its repulsion role in axon guidance and neuronal migration, exerts an inhibitory effect on leukocyte chemotaxis (Wu et al., 2001; Kanellis et al., 2004), suggesting that repulsion by Slit may be a conserved guidance mechanism operative across many cell types.

The present study was undertaken to test the hypothesis that Slit can regulate the recruitment of immune cells in response to proinflammatory stimuli *in vivo*. Intravital microscopy of the cerebral microcirculation was used to measure leukocyte–endothelial adherence (LEA), an early step in leukocyte recruitment, in anesthetized mice (Altay et al., 2004). The proinflammatory stimuli included the cytokine TNFα, as well as global cerebral ischemia, which invokes a broader spectrum of inflammatory mediators. We hypothesized that Slit could alter cell fate indirectly by inhibiting cerebral ischemia-induced leukocyte recruitment and/or directly by exerting cytoprotective effects on neurons and glia, and we evaluated these possibilities both *in vivo* and *in vitro*.

* Corresponding author. Department of Neurosurgery, Box 8057, Washington University School of Medicine, 660 S. Euclid Ave., St. Louis, MO 63110, USA. Fax: +1 314 286 2900.
E-mail address: gidday@wustl.edu (J.M. Gidday).

0014-4886/$ - see front matter. Published by Elsevier Inc.
doi:10.1016/j.expneurol.2007.06.028

Material and methods

Animals

CD-1 male mice (Harlan, Indianapolis, IN) weighing 30–35 g, from 12 to 16 weeks of age, were used. All experimental procedures were approved by our institutional animal studies committee. Mice were anesthetized using chloral hydrate (350 mg/kg, i.p.) and xylazine (4 mg/kg, i.p.).

TNFα protocol

The effect of exogenous Slit on the acute inflammatory response to TNFα was assessed by concomitant administration of TNFα (3.0 μg/kg i.p.) and human Slit protein (3.0 μg/kg, i.p.). Four hours later, animals were anesthetized to measure TNFα-induced leukocyte–endothelial adherence (LEA) to cortical venular endothelium through closed cranial windows (see below). The TNFα-only control group received Slit–Robo vehicle, a serum-free conditioned medium from human embryonic kidney cells. A separate group of mice was concomitantly injected with TNFα and the Slit antagonist RoboN, an extracellular fragment of the Slit receptor (3 μg/kg, i.p.) (Wu et al., 2001), and LEA was measured 4 h later to assess the effects of endogenous Slit on LEA.

Global cerebral ischemia protocol

Anesthetized mice were placed in a supine position on an angled platform, and intubated with a 22-gauge cannula under a surgical microscope; they were ventilated with room air (Harvard Apparatus, model 845) with a stroke volume of 6 ml/kg, at a respiratory rate of 150 breaths per min. Core temperature was maintained at 37 °C with a thermoregulated heating pad. A ventral midline incision was made to expose the common carotid arteries bilaterally, and global ischemia was induced by bilateral common carotid artery occlusion (BCCAO) for 6 min by temporary occlusion of both vessels by Yasargil miniclips. After clip removal, animals were ventilated for an additional 10 min, extubated, and placed in an incubator at 33 °C for 30 min before returning them to their cages. A sham BCCAO control group consisted of mice treated identically except they were not subjected to the carotid occlusion.

To assess whether exogenous Slit exerts effects on the cerebrovascular inflammatory response to global ischemia, we placed an osmotic minipump of 200 μl volume (Alzet, Cupertino, CA) subcutaneously along the animal's back to provide continuous delivery (0.5 μg/kg/h) of compounds of interest for 24 h beginning immediately after BCCAO. Antagonism of endogenous and exogenous Slit was achieved by one pump delivering RoboN, or two separate pumps delivering Slit and RoboN, respectively. Sham BCCAO controls received Slit–Robo vehicle by minipump. LEA was quantified in all animals 24 h after BCCAO. Protein design, purification, and efficacy for Slit and RoboN have been described previously (Kanellis et al., 2004).

The effect of BCCAO on neuronal injury in the vulnerable hippocampal CA1 pyramidal cell region was studied 1 week after BCCAO in separate groups of BCCAO-treated animals with or without Slit or RoboN delivery, and sham BCCAO controls. Continuous administration of Slit or RoboN was achieved by osmotic minipumps, which were placed immediately upon reperfusion, and subsequently replaced daily for three consecutive days.

Cranial window and cerebral blood flow determinations

Four or twenty-four hours after TNFα administration or BCCAO, respectively, animals were anesthetized, tracheostomized through a midline ventral neck approach, and ventilated starting at 6 ml/kg and 150 breaths per minute. Anesthesia was maintained throughout the surgical preparation and imaging procedures by administering supplemental anesthesia as needed. A femoral arterial line was placed for the measurement of blood gases and blood pressure, and rhodamine 6G administration. A blood gas sample was obtained before placing the cranial window, and minor adjustments in tidal volume and/or respiratory rate were made to keep these values within physiological ranges. The animal's head was stabilized in a stereotaxic apparatus, and the right parietal bone was exposed through a scalp incision. Relative measures of cortical cerebral blood flow (CBF) were obtained by laser Doppler flowmetry through the intact bone at 5 different medial and 5 different lateral locations relative to where the cranial window would subsequently be placed to noninvasively assess the effects of TNFα or BCCAO on local CBF. Flow measurements were made under constant, dim ambient light conditions after a 20 s period of stabilization. A 3-mm diameter craniotomy was then performed, leaving the dura intact, and a Plexiglas window was mounted over the opening and sealed to the cranium by dental acrylic. The animal was repositioned on a microscope stage, and regions of the cortical surface exhibiting a heterogeneous pattern of secondary and tertiary arterioles and venules were randomly selected for intravital imaging.

Epifluorescence videomicroscopy for leukocyte dynamics

As described previously (Altay et al., 2004), intravascular leukocyte dynamics (flowing, rolling, and adherence) in cortical venules of anesthetized mice could be visualized using epifluorescence videomicroscopy following *in situ* labeling of circulating leukocytes (lymphocytes and neutrophils) with rhodamine 6G (0.007% in PBS, administered intra-arterially at a rate of 150 μl/min). Leukocyte dynamics were recorded to videotape in real time with the use of a CCD camera (Olympus, 110) mounted on an epifluorescence microscope using a 10× water immersion lens (1.3 NA).

During off-line playback of the video recording, leukocyte–endothelial adherence (LEA) was quantified manually by counting the number of leukocytes adherent to the endothelium of pial venules for longer than 10 consecutive seconds within a user-defined microvessel network that included only secondary and tertiary (20–60 μm diameter) venular branches.

Table 1
Physiological parameters in the TNFα model of cerebrovascular inflammation at 4 h

	n	Age (weeks)	pH	pCO_2 (mm Hg)	pO_2 (mm Hg)	MABP (mm Hg)	Glucose (mg/dl)	CBF	
								Medial	Lateral
Untreated	3	10±0	7.35±0.09	32±7	122±17	64±3	290±60	13±4	9±3
TNFα	9	14±1	7.34±0.02	31±2	118±6	49±4*	293±57	13±1	9±1
TNFα+Slit	6	11±0	7.31±0.02	34±3	106±7	49±2*	206±19	13±2	8±1
TNFα+RoboN	5	12±0	7.34±0.04	30±1	115±12	50±3*	213±11	14±2	10±2
TNFα+Slit veh.	4	14±0	7.30±0.04	32±4	103±7	48±1*	172±27	14±2	9±1

*vs. untreated group.

Histopathology

Animals were euthanized by halothane overdose, and transcardially perfused with heparinized saline. Brains were removed, frozen on dry ice, and stored at −80 °C until the time of sectioning. Sixteen-micron thick coronal sections through the hippocampus were taken starting 1-mm posterior to Bregma; sections were Nissl-stained and post-fixed for histological analyses. Neuronal injury was quantified by light microscopy in three nonadjacent sections from each brain by counting viable pyramidal cells present over a 0.1-mm length in the CA1 region by an observer blinded to the experimental condition, with each hemisphere examined independently. Sections adjacent to those used for Nissl staining were incubated with propidium iodide (2.4 μg/ml of PBS-T) for 10 min, coverslipped, and imaged by fluorescence microscopy for qualitative analysis of BCCAO-induced injury and Slit-mediated protection.

Cell culture

Mixed cultures of neurons and glia were prepared from forebrains of embryonic-day-17 rat fetuses, as previously described (McLaughlin et al., 1998). In brief, dissociated cells were plated on poly-L-ornithine-treated tissue culture plates in a growth medium comprised of 80% Dulbecco's Modified Eagle's Medium (DMEM) (high glucose with L-glutamine and without sodium pyruvate; Gibco/BRL, Grand Island, NY), 10% Ham's F12-Nutrients, and 10% bovine calf serum (heat-inactivated) with 1× antimycotic/antibiotic mixture (with amphotericin B and streptomycin sulfate; Gibco/BRL). Cultures were maintained in an incubator at 37 °C with 5% CO_2.

Oxygen glucose deprivation (OGD) assays were performed on cultures grown for 13–18 days in order to insure they expressed a full compliment of NMDA type glutamate receptors (Legos et al., 2002). Cultures were placed in deoxygenated, glucose-free Earle's balanced salt solution (EBSS) then transferred to an anaerobic chamber (Billups-Rothenberg, Del Mar, CA) containing humidified 95% air/5% CO_2 (control), or humidified 95% N_2/5% CO_2 (anoxic) for 90 min. OGD was terminated by removal of the plate from the chamber, and replacement of the EBSS with oxygenated minimal essential medium containing 0.01% bovine serum albumin. Using both lactate dehydrogenase release and trypan blue exclusion approaches, preliminary experiments determined that none of the purified protein extracts (Slit, RoboN) altered cell viability (data not shown). Purified RoboN was diluted to 1 nmol/l. The Slit protein was used at a final concentration of 1 μg/ml. Proteins were present during the OGD stress and during the 20-h period of reoxygenation/normoglycemia prior to viability assessment by the LDH assay (McLaughlin et al., 2003); cell viability in the experimental cultures was normalized to untreated controls in order to accommodate minor variations in intraculture variability with respect to survival and plating density. To assess whether activated microglial cells were present in our cultures and could have contributed to our results, random samples of both media and cells from cultures exposed to OGD and 20–24 h of reoxygenation/normoglycemia were immunoblotted for OX42, a marker for the CD11b/c complement receptor expressed by activated microglia; cultures were also visually inspected at this time, in a blinded fashion, for the presence of cells showing an activated microglial morphology. In all instances, results of such studies have been negative.

Statistical analysis

Differences in physiological and hemodynamic variables, venular diameter, leukocyte–endothelial adherence, and the

Table 2
Physiological parameters in the BCCAO model of cerebrovascular inflammation at 24 h

	n	Age (weeks)	pH	pCO_2 (mm Hg)	pO_2 (mm Hg)	MABP (mm Hg)	Glucose (mg/dl)	CBF	
								Medial	Lateral
BCCAO sham control	7	13±0	7.36±0.02	27±2	98±7	58±3	266±49	29±7	14±3†
BCCAO	9	14±0	7.33±0.02	29±1	113±5	45±2*	270±45	14±1*†	10±1
BCCAO+Slit	7	12±0	7.31±0.03	30±2	105±8	44±2*	277±44	12±1*†	9±1
BCCAO+RoboN	6	15±1	7.32±0.03	29±3	118±12	43±4*	235±43	13±3*†	12±0
BCCAO+Slit+RoboN	8	13±0	7.36±0.02	28±2	104±9	61±8	202±26	14±2*†	14±2†
BCCAO+Slit vehicle	5	13±0	7.33±0.02	30±2	114±10	38±1*	261±28	9±0*	8±1

*vs. BCCAO sham control.
†vs. BCCAO+Slit vehicle.

histopathological data within and between groups were assessed by nonparametric repeated-measures ANOVA, using Mann–Whitney's rank sum test; Bonferroni multiple comparisons test was used for the cell culture LDH data. A p-value less than 0.05 was considered statistically significant.

Results

Physiologic and hemodynamic variables

Animals that received TNFα had significantly lower mean arterial blood pressures at 4 h compared to untreated controls (Table 1). Similarly, animals subjected to BCCAO tended to have lower blood pressures at 24 h compared to sham animals (Table 2). No significant differences were noted in arterial blood gases and glucose values within or between groups in the TNFα-treated mice, as well as within or between groups in the BCCAO-treated mice, at 4 h and 24 h, respectively (Tables 1 and 2).

Cerebral blood flow

Baseline CBF tended to be higher medially than laterally, consistent with regional differences in the distribution of pre- and postcapillary microcirculatory vessels as well as the progressively larger venules draining medially into the sagittal sinus. In a separate group of animals, no difference in baseline CBF was observed between the right and the left hemisphere in animals with bilateral craniotomy (data not shown). Medial and lateral CBF remained unchanged among all TNFα-treated animals (Table 1), but both tended to be reduced in animals subjected to BCCAO relative to sham BCCAO controls (Table 2). There were no significant differences in the maximum or minimum venular diameters, or in the total areas of the defined venular network, in which leukocyte adherence was determined, in the different groups (data not shown).

Leukocyte–endothelial adherence (LEA)

A dose-dependent increase in LEA to cortical venular endothelium was observed 4 h after systemic TNFα administration at doses of 1.5, 3.0, and 15.0 μg/kg (Fig. 1, inset; $n=22$). In two other groups, we assessed the effects of exogenous and endogenous Slit on LEA induced by a high dose (3.0 μg/kg) and moderate dose (1.5 μg/kg) of TNFα, respectively. The 35-fold increase in LEA ($p=0.017$) induced by the high dose of TNFα ($n=7$) was virtually completely blocked (98%; $p=0.001$) in the presence of Slit ($n=6$). Conversely, the TNFα-induced 16-fold increase in LEA ($p=0.012$) in response to the moderate dose was significantly exacerbated ($p=0.011$) in animals treated with RoboN, the soluble receptor for Slit ($n=5$; Fig. 1). Slit–Robo vehicle did not have any effect on TNF-induced LEA.

In animals subjected to BCCAO ($n=9$), a significant, four-fold increase ($p=0.001$) in LEA was measured at 24 h of reperfusion, relative to that noted in sham BCCAO controls ($n=7$). This postischemic inflammatory response was inhibited by 79% ($p=0.003$) in animals administered Slit ($n=7$). Administration of the Slit–Robo vehicle ($n=5$) was without effect on BCCAO-induced increases in LEA. Unlike the response to RoboN observed in TNFα-treated mice, RoboN did not affect the comparable elevation in LEA induced by global ischemia (Fig. 2). However, when administered simultaneously with Slit, RoboN reversed Slit's anti-inflammatory effect on BCCAO-induced LEA (Fig. 2).

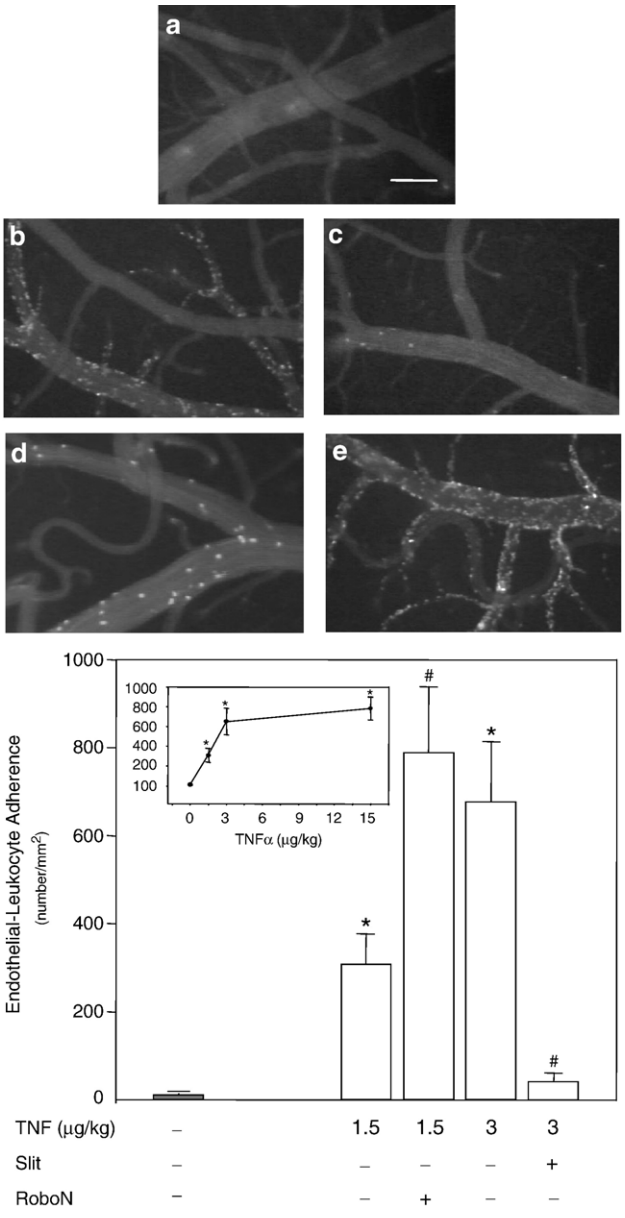

Fig. 1. Effect of Slit on TNFα-induced increases in leukocyte–endothelial adherence. Representative epifluorescent videophotomicrographs of cortical venular leukocytes in the different groups are shown, relative to untreated controls (a). TNFα (3 μg/kg) induced leukocyte adherence to cerebral venular endothelium (b) and this response was completely blocked by exogenous Slit (c). The increase in leukocyte–endothelial adherence induced by TNFα (1.5 μg/kg) (d) was exacerbated by the soluble receptor RoboN (e), reflecting tonic inhibition of adherence by endogenous Slit. Histogram summarizes the magnitude of leukocyte–endothelial adherence under the different experimental conditions, relative to naive controls (shaded bar). Inset: Dose dependency of TNFα-induced inflammation. Intravital imaging was performed 4 h after animals were administered TNFα. *$p<0.05$ vs. sham; #$p<0.05$ vs. TNFα only (at the corresponding dose). Scale bar=100 μm.

In vivo neuronal injury

In keeping with previous findings (Barone et al., 1993), significant (~50%) pyramidal cell death occurred in the CA1 region of dorsal hippocampus in mice subjected to 6 min of BCCAO. Dead and dying pyramidal cells in the injured hippocampi displayed features of cellular necrosis, characterized in Nissl-stained coronal sections by pyknotic nuclei, irregular cell contours, and loss of nuclear dye retention. Moreover, intense labeling of pyramidal cell nuclei with propidium iodide was detected on adjacent thin sections. In Slit-treated mice, the extent of BCCAO-induced hippocampal CA1 pyramidal cell loss was significantly diminished relative to untreated animals ($p=0.025$; Fig. 3).

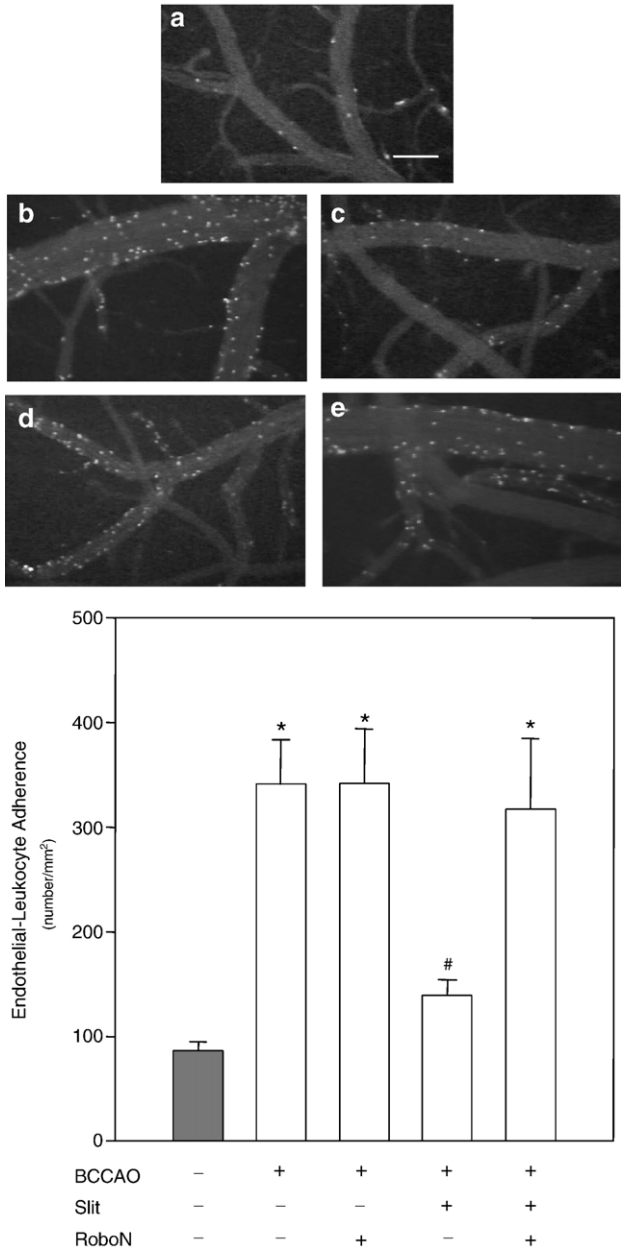

Fig. 2. Effect of Slit on increases in leukocyte–endothelial adherence induced by global ischemia (bilateral common carotid occlusion [BCCAO]). Representative epifluorescent videophotomicrographs of cortical venular leukocytes in the different groups are shown, relative to sham BCCAO controls (a). BCCAO-induced leukocyte adherence to cerebral venular endothelium (b) was blocked by co-administration of Slit (c). The soluble receptor RoboN blocked Slit's inhibitory effect on BCCAO-induced adherence (d) but did not exacerbate BCCAO-induced adherence (e). Histogram summarizes the magnitude of leukocyte–endothelial adherence under the different experimental conditions, relative to naive controls (shaded bar). Animals received 6 min BCCAO and recovered 24 h before intravital imaging of leukocyte–endothelial adherence. *$p<0.05$ vs. sham; #$p<0.05$ vs. BCCAO. Scale bar=100 μm.

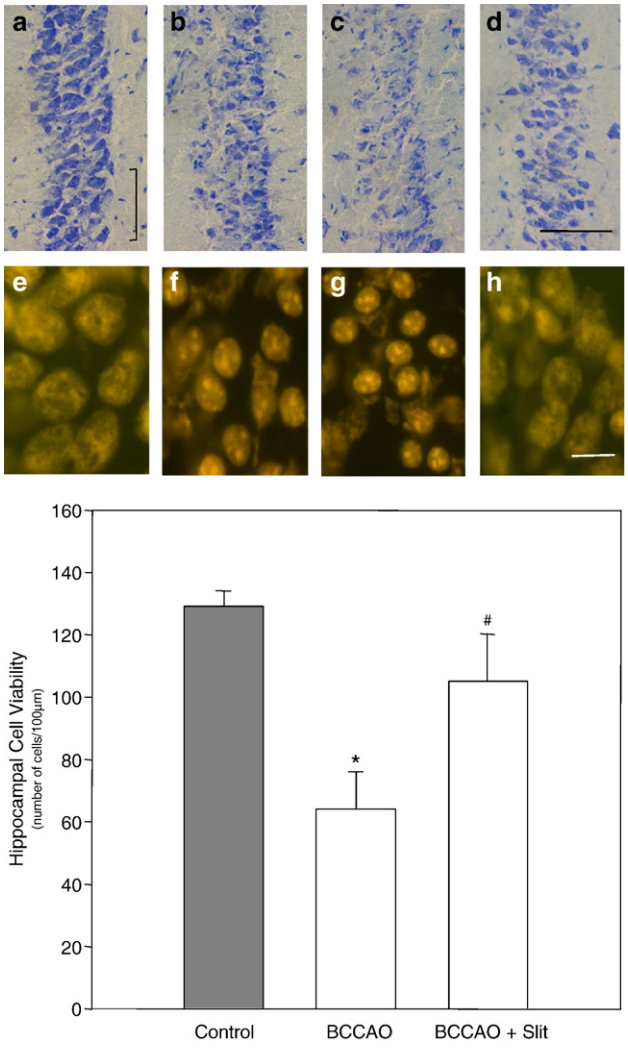

Fig. 3. Effect of Slit on CA1 pyramidal cell injury following global ischemia. Representative Nissl-stained (a-d, first row) and propidium iodide-stained (e–h, second row) hippocampal CA1 pyramidal cells 7 days after global ischemia (bilateral common carotid occlusion [BCCAO]). Relative to naive controls (a, e), in animals with both moderate (~50% cell loss; b, f) and severe (~80% cell loss; c, g) CA1 injury, PI-labeled cells displayed distinct, multiple, hyperintense nuclear condensations. However, in animals treated with Slit (d, h), a more viable pyramidal cell morphology was the prominent feature. The histogram quantifies the protective effect of exogenous Slit on hippocampal CA1 pyramidal cell viability, relative to naive controls (shaded bar). *$p<0.05$ vs. control; #$p<0.05$ vs. BCCAO. Scale bar=50 μm and 10 μm in Nissl- and PI-stained sections, respectively.

In vitro neuronal injury

Ninety-minute OGD and 20-h reoxygenation under normoglycemic conditions caused a substantial amount ($p<0.001$) of

neuronal cell death in mixed cultures, characterized by neurite beading and retraction, cellular vacuolization, loss of membrane integrity, cellular debris, and release of LDH from dead and dying cells (Fig. 4). This injury was completely inhibited by Slit (Fig. 4; $p<0.001$). RoboN reversed the Slit effect when co-incubated in the cultures subjected to OGD (Fig. 4; $p<0.001$).

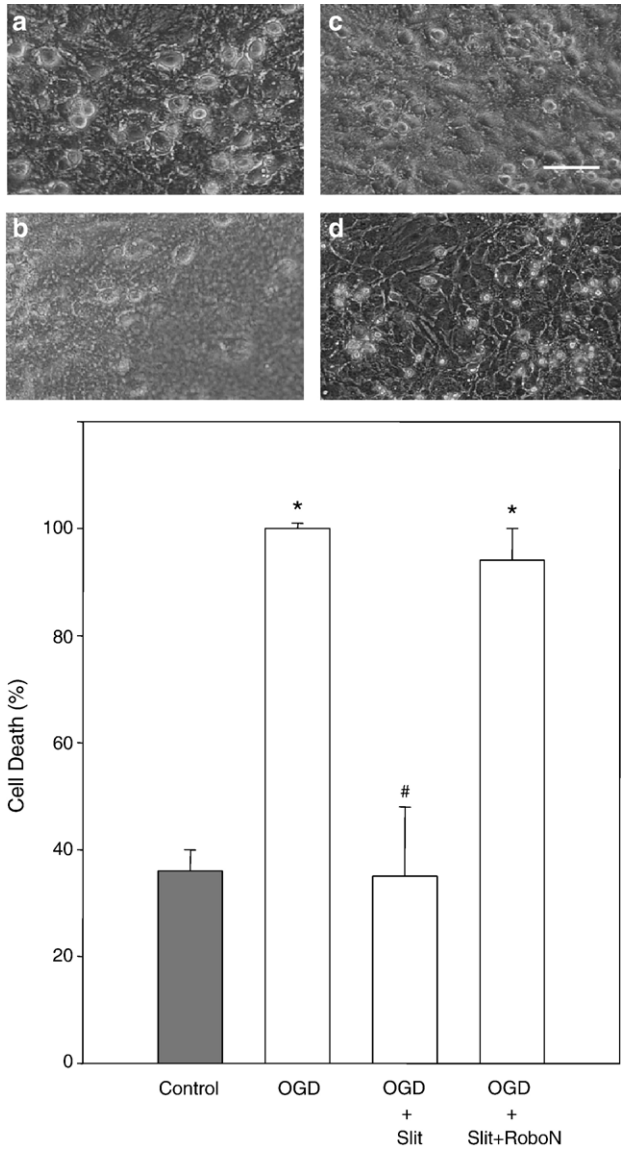

Fig. 4. Effects of Slit on oxygen–glucose deprivation (OGD)/reoxygenation injury in mixed neuronal–glial cultures. Representative photomicrographs are provided for each experimental condition. (a) Under untreated control conditions, neurons were healthy, phase bright, and had well defined processes. (b) Ninety-minute OGD resulted in robust neuronal cell death with marked cellular debris evident the following day. (c) Slit significantly and dramatically attenuated neuronal cell death induced by 90-min OGD and recovery. Although some morphological changes occurred, including slight decreases in cell volume, neurons remained viable (as assessed by LDH assay). (d) The protective effect of Slit was reversed by co-incubation with its soluble receptor RoboN. Histogram shows quantification of neuronal cell death as assessed by release of lactate dehydrogenase (LDH) into the media, normalized to total kill (100%), relative to naive, untreated controls (shaded bar) over the same time period. *$p<0.001$ vs. control; #$p<0.001$ vs. OGD. Scale bar=40 μm.

Vehicle treatment had no effect on neuronal death or survival following OGD in this model (data not shown).

Discussion

Based on studies in a variety of cell guidance models, the ability of the peptide Slit to repel migrating neurons is well established (Guan and Rao, 2003). Recently, a similar repellent effect of Slit against immune cells was demonstrated *in vitro* in human embryonic kidney cells (Wu et al., 2001), and in a rat model of glomerulonephritis (Kanellis et al., 2004), suggesting that this peptide may serve as a universal negative regulator of cell migration (Rao et al., 2002). The present results are the first to demonstrate *in vivo* that Slit modulates cerebrovascular inflammatory responses, using TNFα and global ischemia as distinct proinflammatory stimuli. This effect was manifested by a reduction in leukocyte adherence to the cortical venular endothelium 4 h after TNFα treatment and 24 h after cerebral ischemia in adult mice. The exacerbation of TNFα-induced cerebrovascular inflammation in response to inhibition of endogenous Slit with RoboN, its soluble receptor, reveals the ability of endogenously secreted Slit to suppress leukocyte recruitment in brain. In addition to documenting anti-inflammatory effects *in vivo*, the present study is the first to provide *in vivo* and *in vitro* evidence that Slit is neuroprotective. Specifically, Slit abrogated the delayed cell death in hippocampal CA1 pyramidal neurons following global ischemia, and reduced neuronal cell death in mixed neuronal–glial cultures subjected to simulated ischemia; the latter findings demonstrate that this protective effect is, at least in part, due to direct effects of Slit on neurons and/or on neuron–glial interactions, and not solely the indirect result of Slit's ability to reduce postischemic inflammation.

Leukocyte adhesion to vascular endothelium occurs via highly specific receptor–ligand interactions between leukocytes, endothelium, and extravascular matrix (Springer, 1990). The requisite first step involves the low-affinity "rolling" of the leukocyte on the endothelium through the engagement of selectins (E-, P-, and L-selectin) with their ligands, PSGL-1 and sialyl LewisX, followed by a high-affinity "firm" adhesion mediated by leukocyte integrins binding to the endothelial intercellular adhesion molecule (ICAM-1) (Alon et al., 2003). The cytoplasmic domains of the integrins, selectins, and ICAM-1 are linked to the cytoskeleton through adapter actin-binding proteins, allowing for direct associations between integrins and cytoskeletal function (Sampath et al., 1998; Yoshida et al., 1996; Carpen et al., 1992). The intracellular mechanisms by which Slit negatively regulated leukocyte–endothelial dynamics in the cerebral microcirculation were not investigated in the present study, but available evidence supports the following sequence of events: Slit interaction with the extracellular domain of its single transmembrane domain receptor Robo promotes an association of the Slit–Robo complex with a novel family of Rho GTPase-activating proteins (GAPs) forming Slit–Robo GAPs (srGAPs) (Wong et al., 2001). srGAPs in turn become associated with Rho GTPases (Wong et al., 2001) that regulate cellular polarization and actin cytoskeletal changes in neutrophils during chemotaxis (Xu et al., 2003). The interaction between srGAPs and Rho

GTPases changes the relative balance between the active and inactive Rho GTPase forms, and abolishes the directional mobility of the cell towards chemoattractants (Wong et al., 2001). In addition to the leukocyte-based mechanism outlined above, Slit might exert its anti-chemotactic effect by negative regulation of Rho GTPase signaling in endothelial cells, which also express Slit receptors (Park et al., 2003; Wang et al., 2003). The inhibition of Rho-mediated cascades by Slit engagement of these receptors could lead to increased expression and activity of endothelial nitric oxide synthase (Laufs et al., 2000), a potent anti-inflammatory mediator (Altay et al., 2004; Kubes et al., 1991), and decreased ICAM-1-mediated signaling (Adamson et al., 1999) within the endothelial cell.

We tested the ability of Slit to modulate chemotaxis in the *in vivo* brain using two different proinflammatory stimuli: the cytokine TNFα (Carvalho-Tavares et al., 2000), and transient global ischemia, in which TNFα derived from resident cells (Liu et al., 1994; Gregersen et al., 2000; Botchkina et al., 1997; Uno et al., 1997; Feuerstein et al., 1998) and mediators of other inflammatory signaling cascades promotes postischemic inflammation in the postcapillary venular system and in cerebral parenchyma. In both models, we found exogenously administered Slit to be potently effective in reducing cerebrovascular inflammation. The involvement of endogenously produced Slit in modulating leukocyte chemotaxis was revealed by our finding that antagonism of endogenous Slit activity by RoboN administration exacerbated TNFα-induced LEA. This finding suggests that endogenous Slit may participate in counteracting the pro-inflammatory effects of constitutively produced TNFα and other cytokines which, under basal conditions, may allow them to act as neuromodulators (Vitkovic et al., 2000). The lack of exacerbation of the cerebrovascular inflammatory response to global ischemia by RoboN has several possible explanations. Slit's leukocyte modulatory effects may be more limited in situations wherein multiple proinflammatory mediators are present, which is likely to occur with global ischemia (Saito et al., 1996; Jander et al., 2000; Panahian et al., 1996; Matsumoto et al., 1997; Zhu et al., 2006). Secondly, because of differences in the timecourse of the inflammatory responses triggered by systemically administered TNFα, and that induced following global ischemia, which can involve multiple peaks in TNFα expression (Zhu et al., 2006), and given differences in Slit dose and route of administration in the two models we studied, we surmise that we could be witnessing a model and/or timecourse dependency. Global ischemia might also lead to the inhibition of Slit synthesis and/or constitutive production of Slit, such that the RoboN we administered had no ligand on which to bind.

The present study provides the first *in vivo* evidence of neuroprotection by Slit against ischemic injury of hippocampal CA1 pyramidal neurons. This effect may have resulted indirectly from a Slit-induced decrease in leukocyte chemotaxis and recruitment, and/or directly from a Slit-induced change in the neuronal response to ischemia. Although not a universal finding (Hayward et al., 1996; Emerich et al., 2002), considerable evidence supports the notion that adherent and infiltrating leukocytes contribute to ischemic damage following focal ischemia (see Jean et al., 1998; Wang et al., 2007; Zheng and Yenari, 2004 for reviews). In particular, the degree of leukocyte infiltration following focal stroke correlates with the severity of neuronal injury and neurological deficits in animals (Zhang et al., 1994a,b; Clark et al., 1994; del Zoppo et al., 1991) and humans (Akopov et al., 1996). Moreover, in focal ischemia models, anti-leukocyte interventions decrease cerebral edema (Strachan et al., 1992), improve cerebral blood flow (Grogaard et al., 1989; Connolly et al., 1996; Ishikawa et al., 2004), and reduce infarct size (Connolly et al., 1996; Zhang et al., 1994a,b; Chopp et al., 1994; Xu et al., 2004). Finally, adhesion molecule knockout mice consistently exhibit smaller lesion volumes following focal stroke than their wild-type counterparts (Prestigiacomo et al., 1999; Soriano et al., 1996). The evidence for leukocytes contributing to neuronal injury following global cerebral ischemia is not as robust, in part because considerably fewer studies have been conducted relative to focal stroke. Several interventions that directly or indirectly reduce inflammation improve outcome in the setting of global ischemia (Lee et al., 1999; Block et al., 2001; Ueda and Nowak, 2005). On the other hand, leukocyte-directed therapies do not always provide benefit in global ischemia models (Aspey et al., 1989; Schott et al., 1989; Emerich et al., 2002).

Thus, to investigate whether direct protective effects of Slit accounted for the neuroprotection we measured in Slit-treated animals following global ischemia, independent of an anti-inflammatory effect, we exposed mixed neuronal–glial cultures to simulated ischemia as a mimic of the *in vivo* condition. Slit's ability to protect against neuronal injury in this model, the first demonstration of its kind that we are aware of, must result from Slit-mediated signaling of cytoprotective pathways in glia and/or neurons independent of any reduction in leukocyte chemotaxis. Although further studies are required to elucidate the mechanistic basis for the observed protective effect, a direct effect of Slit that improves the glial response to ischemia is possible, since the ability of glial cells to promote neuronal viability in the setting of ischemia is well established (Lee et al., 2004; Rosenberg and Aizenman, 1989; Heidinger et al., 1999; Trendelenburg and Dirnagl, 2005; Swanson et al., 2004). In *Drosophila*, glial Slit receptors play an important role in neuron–glia interactions by influencing the survival and migration of both cell types; moreover, interfering with these interactions alters their responsiveness to Slit–Robo signaling (Kinrade et al., 2001). Slit might also exert a direct neuroprotective effect through its association with Rho GTPase-mediated cytoskeletal rearrangements to stabilize the cellular architecture of the neuron itself. In particular, there is substantial evidence that Rho GTPases are involved in synaptic remodeling and maintenance (Govek et al., 2005), and relative changes in their active/inactive state are associated with dendritic plasticity (Nakayama et al., 2000; Pilpel and Segal, 2004). Moreover, inhibition of Rho GTPases or their effectors protects against ischemia/reperfusion injury *in vivo* in both brain (Laufs et al., 2000; Trapp et al., 2001) and other tissues (Bao et al., 2004). Based on these findings, we offer the speculation that modulation of Rho GTPase signaling cascades by Slit has the net effect of maintaining cellular integrity and function in ischemic brain secondary to its ability to

prevent or reduce synaptic disruption and other changes in dendritic morphology crucial to neuronal viability (Hasbani et al., 2001; Park et al., 1996).

In conclusion, our studies reveal that endogenous Slit negatively modulates cerebrovascular inflammatory responses. Both cytokine-induced and ischemia-induced leukocyte recruitment in the cerebral microcirculation could be attenuated by exogenous Slit. Slit-treated animals also exhibited a reduction in hippocampal pyramidal cell loss following global ischemia, consistent with our demonstration of a Slit-mediated neuroprotective effect in mixed neuronal–glial cultures subjected to simulated ischemia. Future studies are required to enhance our understanding of how Slit functions at the molecular level to reduce leukocyte recruitment and neuronal injury in ischemic brain, and the extent to which the reduction in CA1 pyramidal cell injury was secondary to the anti-chemotactic effects of Slit. Nevertheless, our findings suggest that modulation of Slit levels and/or activity may serve as a therapeutic strategy for a wide spectrum of diseases characterized by cerebrovascular inflammation and/or neuronal injury.

Acknowledgments

We thank Rebecca Sams for excellent technical assistance, and Yolanda M. Rangel PhD for critical reading of the manuscript. This work was supported by NIH grants HL66360 (JMG), NS21045 (TSP), CA114197 (JYW), NICHD P30HD15052 (BAM), NS50396 (BAM), the Leukemia and Lymphoma Society (JYW), and the Spastic Paralysis Research Foundation of the Illinois-Eastern Iowa District of Kiwanis International (TSP).

References

Adamson, P., Etienne, S., Couraud, P.O., Calder, V., Greenwood, J., 1999. Lymphocyte migration through brain endothelial cell monolayers involves signaling through endothelial ICAM-1 via a rho-dependent pathway. J. Immunol. 162, 2964–2973.

Akopov, S.E., Simonian, N.A., Grigorian, G.S., 1996. Dynamics of polymorphonuclear leukocyte accumulation in acute cerebral infarction and their correlation with brain tissue damage. Stroke 27, 1739–1743.

Alon, R., Grabovsky, V., Feigelson, S., 2003. Chemokine induction of integrin adhesiveness on rolling and arrested leukocytes local signaling events or global stepwise activation? Microcirculation 10, 297–311.

Altay, T., Gonzales, E.R., Park, T.S., Gidday, J.M., 2004. Cerebrovascular inflammation after brief episodic hypoxia: modulation by neuronal and endothelial nitric oxide synthase. J. Appl. Physiol. 96, 1223–1230.

Aspey, B.S., Jessimer, C., Pereira, S., Harrison, M.J., 1989. Do leukocytes have a role in the cerebral no-reflow phenomenon? J. Neurol. Neurosurg. Psychiatr. 52, 526–528.

Bao, W., Hu, E., Tao, L., Boyce, R., Mirabile, R., Thudium, D.T., Ma, X.L., Willette, R.N., Yue, T.L., 2004. Inhibition of Rho-kinase protects the heart against ischemia/reperfusion injury. Cardiovasc. Res. 61, 548–558.

Barone, F.C., Knudsen, D.J., Nelson, A.H., Feuerstein, G.Z., Willette, R.N., 1993. Mouse strain differences in susceptibility to cerebral ischemia are related to cerebral vascular anatomy. J. Cereb. Blood Flow Metab. 13, 683–692.

Block, F., Bozdag, I., Nolden-Koch, M., 2001. Inflammation contributes to the postponed ischemic neuronal damage following treatment with a glutamate antagonist in rats. Neurosci. Lett. 298, 103–106.

Blond, D., Campbell, S.J., Butchart, A.G., Perry, V.H., Anthony, D.C., 2002. Differential induction of interleukin-1beta and tumour necrosis factor-alpha may account for specific patterns of leukocyte recruitment in the brain. Brain Res. 958, 89–99.

Botchkina, G.I., Meistrell III, M.E., Botchkina, I.L., Tracey, K.J., 1997. Expression of TNF and TNF receptors (p55 and p75) in the rat brain after focal cerebral ischemia. Mol. Med. 3, 765–781.

Carpen, O., Pallai, P., Staunton, D.E., Springer, T.A., 1992. Association of intercellular adhesion molecule-1 (ICAM-1) with actin-containing cytoskeleton and alpha-actinin. J. Cell Biol. 118, 1223–1234.

Cartier, L., Hartley, O., Dubois-Dauphin, M., Krause, K.H., 2005. Chemokine receptors in the central nervous system: role in brain inflammation and neurodegenerative diseases. Brain Res. Brain Res. Rev. 48, 16–42.

Carvalho-Tavares, J., Hickey, M.J., Hutchison, J., Michaud, J., Sutcliffe, I.T., Kubes, P., 2000. A role for platelets and endothelial selectins in tumor necrosis factor-alpha-induced leukocyte recruitment in the brain microvasculature. Circ. Res. 87, 1141–1148.

Chopp, M., Zhang, R.L., Chen, H., Li, Y., Jiang, N., Rusche, J.R., 1994. Postischemic administration of an anti-Mac-1 antibody reduces ischemic cell damage after transient middle cerebral artery occlusion in rats. Stroke 25, 869–875.

Clark, R.K., Lee, E.V., White, R.F., Jonak, Z.L., Feuerstein, G.Z., Barone, F.C., 1994. Reperfusion following focal stroke hastens inflammation and resolution of ischemic injured tissue. Brain Res. Bull. 35, 387–392.

Connolly Jr., E.S., Winfree, C.J., Springer, T.A., Naka, Y., Liao, H., Yan, S.D., Stern, D.M., Solomon, R.A., Gutierrez-Ramos, J.C., Pinsky, D.J., 1996. Cerebral protection in homozygous null ICAM-1 mice after middle cerebral artery occlusion. Role of neutrophil adhesion in the pathogenesis of stroke. J. Clin. Invest. 97, 209–216.

del Zoppo, G.J., Schmid-Schonbein, G.W., Mori, E., Copeland, B.R., Chang, C.M., 1991. Polymorphonuclear leukocytes occlude capillaries following middle cerebral artery occlusion and reperfusion in baboons. Stroke 22, 1276–1283.

del Zoppo, G., Ginis, I., Hallenbeck, J.M., Iadecola, C., Wang, X., Feuerstein, G.Z., 2000. Inflammation and stroke: putative role for cytokines, adhesion molecules and iNOS in brain response to ischemia. Brain Pathol. 10, 95–112.

Emerich, D.F., Dean, R.L., Bartus, R.T., 2002. The role of leukocytes following cerebral ischemia: pathogenic variable or bystander reaction to emerging infarct? Exp. Neurol. 173, 168–181.

Feuerstein, G., Wang, X., Barone, F.C., 1998. Cytokines in brain ischemia-the role of TNF alpha. Cell. Mol. Neurobiol. 18, 695–701.

Govek, E.E., Newey, S.E., Van Aelst, L., 2005. The role of the Rho GTPases in neuronal development. Genes Dev. 19, 1–49.

Gregersen, R., Lambertsen, K., Finsen, B., 2000. Microglia and macrophages are the major source of tumor necrosis factor in permanent middle cerebral artery occlusion in mice. J. Cereb. Blood Flow Metab. 20, 53–65.

Grogaard, B., Schurer, L., Gerdin, B., Arfors, K.E., 1989. Delayed hypoperfusion after incomplete forebrain ischemia in the rat. The role of polymorphonuclear leukocytes. J. Cereb. Blood Flow Metab. 9, 500–505.

Guan, K.L., Rao, Y., 2003. Signalling mechanisms mediating neuronal responses to guidance cues. Nat. Rev., Neurosci. 4, 941–956.

Hasbani, M.J., Viquez, N.M., Goldberg, M.P., 2001. NMDA receptors mediate hypoxic spine loss in cultured neurons. NeuroReport 12, 2731–2735.

Hayward, N.J., Elliott, P.J., Sawyer, S.D., 1996. Lack of evidence for neutrophil participation during infarct formation focal cerebral ischemia in the rat. Exp. Neurol. 139, 188–202.

Heidinger, V., Hicks, D., Sahel, J., Dreyfus, H., 1999. Ability of retinal Muller glial cells to protect neurons against excitotoxicity in vitro depends upon maturation and neuron-glial interactions. Glia 25, 229–239.

Ishikawa, M., Zhang, J.H., Nanda, A., Granger, D.N., 2004. Inflammatory responses to ischemia and reperfusion in the cerebral microcirculation. Front. Biosci. 9, 1339–1347.

Jander, S., Schroeter, M., Stoll, G., 2000. Role of NMDA receptor signaling in the regulation of inflammatory gene expression after focal brain ischemia. J. Neuroimmunol. 109, 181–187.

Jean, W.C., Spellman, S.R., Nussbaum, E.S., Low, W.C., 1998. Reperfusion injury after focal cerebral ischemia: the role of inflammation and the therapeutic horizon. Neurosurgery 43, 1382–1396.

Kanellis, J., Garcia, G.E., Li, P., Parra, G., Wilson, C.B., Rao, Y., Han, S., Smith,

C.W., Johnson, R.J., Wu, J.Y., Feng, L., 2004. Modulation of inflammation by slit protein in vivo in experimental crescentic glomerulonephritis. Am. J. Pathol. 165, 341–352.

Kinrade, E.F., Brates, T., Tear, G., Hidalgo, A., 2001. Roundabout signalling, cell contact and trophic support confine longitudinal glia and axons in the *Drosophila* CNS. Development 128, 207–216.

Kubes, P., Suzuki, M., Granger, D.N., 1991. Nitric oxide: an endogenous modulator of leukocyte adhesion. Proc. Natl. Acad. Sci. U. S. A. 88, 4651–4655.

Laufs, U., Endres, M., Stagliano, N., Amin-Hanjani, S., Chui, D.S., Yang, S.X., Simoncini, T., Yamada, M., Rabkin, E., Allen, P.G., Huang, P.L., Bohm, M., Schoen, F.J., Moskowitz, M.A., Liao, J.K., 2000. Neuroprotection mediated by changes in the endothelial actin cytoskeleton. J. Clin. Invest. 106, 15–24.

Lee, H.W., Koo, H., Choi, K.G., Park, K.D., Lee, B.C., 1999. The effects of peripheral leukocytes on the hippocampal neuronal changes in transient global ischemia and unilateral cerebral hemispheric infarction. J. Korean Med. Sci. 14, 304–314.

Lee, Y., Aono, M., Laskowitz, D., Warner, D.S., Pearlstein, R.D., 2004. Apolipoprotein E protects against oxidative stress in mixed neuronal–glial cell cultures by reducing glutamate toxicity. Neurochem. Int. 44, 107–118.

Legos, J.J., McLaughlin, B., Skaper, S.D., Strijbos, P.J., Parsons, A.A., Aizenman, E., Herin, G.A., Barone, F.C., Erhardt, J.A., 2002. The selective p38 inhibitor SB-239063 protects primary neurons from mild to moderate excitotoxic injury. Eur. J. Pharmacol. 447, 37–42.

Liu, T., Clark, R.K., McDonnell, P.C., Young, P.R., White, R.F., Barone, F.C., Feuerstein, G.Z., 1994. Tumor necrosis factor-alpha expression in ischemic neurons. Stroke 25, 1481–1488.

Matsumoto, T., Ikeda, K., Mukaida, N., Harada, A., Matsumoto, Y., Yamashita, J., Matsushima, K., 1997. Prevention of cerebral edema and infarct in cerebral reperfusion injury by an antibody to interleukin-8. Lab. Invest. 77, 119–125.

McLaughlin, B., Hartnett, K.A., Erhardt, J.A., Legos, J.J., White, R.F., Barone, F.C., Aizenman, E., 2003. Caspase 3 activation is essential for neuroprotection in preconditioning. Proc. Nat. Acad. Sci. 100, 715–720.

McLaughlin, B.A., Nelson, D., Silver, I.A., Erecinska, M., Chesselet, M.F., 1998. Methylmalonate toxicity in primary neuronal cultures. Neuroscience 86, 279–290.

Nakayama, A.Y., Harms, M.B., Luo, L., 2000. Small GTPases Rac and Rho in the maintenance of dendritic spines and branches in hippocampal pyramidal neurons. J. Neurosci. 20, 5329–5338.

Panahian, N., Yoshida, T., Huang, P.L., Hedley-Whyte, E.T., Dalkara, T., Fishman, M.C., Moskowitz, M.A., 1996. Attenuated hippocampal damage after global cerebral ischemia in mice mutant in neuronal nitric oxide synthase. Neuroscience 72, 343–354.

Park, J.S., Bateman, M.C., Goldberg, M.P., 1996. Rapid alterations in dendrite morphology during sublethal hypoxia or glutamate receptor activation. Neurobiol. Dis. 3, 215–227.

Park, K.W., Morrison, C.M., Sorensen, L.K., Jones, C.A., Rao, Y., Chien, C.B., Wu, J.Y., Urness, L.D., Li, D.Y., 2003. Robo4 is a vascular-specific receptor that inhibits endothelial migration. Dev. Biol. 261, 251–267.

Pilpel, Y., Segal, M., 2004. Activation of PKC induces rapid morphological plasticity in dendrites of hippocampal neurons via Rac and Rho-dependent mechanisms. Eur. J. Neurosci. 19, 3151–3164.

Prestigiacomo, C.J., Kim, S.C., Connolly Jr., E.S., Liao, H., Yan, S.F., Pinsky, D.J., 1999. CD18-mediated neutrophil recruitment contributes to the pathogenesis of reperfused but not nonreperfused stroke. Stroke 30, 1110–1117.

Rao, Y., Wong, K., Ward, M., Jurgensen, C., Wu, J.Y., 2002. Neuronal migration and molecular conservation with leukocyte chemotaxis. Genes Dev. 16, 2973–2984.

Rosenberg, P.A., Aizenman, E., 1989. Hundred-fold increase in neuronal vulnerability to glutamate toxicity in astrocyte-poor cultures of rat cerebral cortex. Neurosci. Lett. 103, 162–168.

Saito, K., Suyama, K., Nishida, K., Sei, Y., Basile, A.S., 1996. Early increases in TNF-alpha, IL-6 and IL-1 beta levels following transient cerebral ischemia in gerbil brain. Neurosci. Lett. 206, 149–152.

Sampath, R., Gallagher, P.J., Pavalko, F.M., 1998. Cytoskeletal interactions with the leukocyte integrin beta2 cytoplasmic tail. Activation-dependent regulation of associations with talin and alpha-actinin. J. Biol. Chem. 273, 33588–33594.

Schott, R.J., Natale, J.E., Ressler, S.W., Burney, R.E., D'Alecy, L.G., 1989. Neutrophil depletion fails to improve neurologic outcome after cardiac arrest in dogs. Ann. Emerg. Med. 18, 517–522.

Soriano, S.G., Lipton, S.A., Wang, Y.F., Xiao, M., Springer, T.A., Gutierrez-Ramos, J.C., Hickey, P.R., 1996. Intercellular adhesion molecule-1-deficient mice are less susceptible to cerebral ischemia-reperfusion injury. Ann. Neurol. 39, 618–624.

Springer, T.A., 1990. Adhesion receptors of the immune system. Nature 346, 425–434.

Stanimirovic, D., Satoh, K., 2000. Inflammatory mediators of cerebral endothelium: a role in ischemic brain inflammation. Brain Pathol. 10, 113–126.

Strachan, R.D., Kane, P.J., Cook, S., Chambers, I.R., Clayton, C.B., Mendelow, A.D., 1992. Immunosuppression by whole-body irradiation and its effect on oedema in experimental cerebral ischaemia. Acta Neurol. Scand. 86, 256–259.

Swanson, R.A., Ying, W., Kauppinen, T.M., 2004. Astrocyte influences on ischemic neuronal death. Curr. Mol. Med. 4, 193–205.

Trapp, T., Olah, L., Holker, I., Besselmann, M., Tiesler, C., Maeda, K., Hossmann, K.A., 2001. GTPase RhoB: an early predictor of neuronal death after transient focal ischemia in mice. Mol. Cell. Neurosci. 17, 883–894.

Trendelenburg, G., Dirnagl, U., 2005. Neuroprotective role of astrocytes in cerebral ischemia: focus on ischemic preconditioning. Glia 50, 307–320.

Ueda, M., Nowak Jr., T.S., 2005. Protective preconditioning by transient global ischemia in the rat: components of delayed injury progression and lasting protection distinguished by comparisons of depolarization thresholds for cell loss at long survival times. J. Cereb. Blood Flow Metab. 25, 949–958.

Uno, H., Matsuyama, T., Akita, H., Nishimura, H., Sugita, M., 1997. Induction of tumor necrosis factor-alpha in the mouse hippocampus following transient forebrain ischemia. J. Cereb. Blood Flow Metab. 17, 491–499.

Vitkovic, L., Bockaert, J., Jacque, C., 2000. Inflammatory cytokines: neuromodulators in normal brain? J. Neurochem. 74, 457–471.

Wang, B., Xiao, Y., Ding, B.B., Zhang, N., Yuan, X., Gui, L., Qian, K.X., Duan, S., Chen, Z., Rao, Y., Geng, J.G., 2003. Induction of tumor angiogenesis by Slit–Robo signaling and inhibition of cancer growth by blocking Robo activity. Cancer Cell 4, 19–29.

Wang, Q., XN Tang, X.N., Yenari, M.A., 2007. The inflammatory response in stroke. J. Neuroimmunol. 184, 53–68.

Wong, K., Ren, X.R., Huang, Y.Z., Xie, Y., Liu, G., Saito, H., Tang, H., Wen, L., Brady-Kalnay, S.M., Mei, L., Wu, J.Y., Xiong, W.C., Rao, Y., 2001. Signal transduction in neuronal migration: roles of GTPase activating proteins and the small GTPase Cdc42 in the Slit–Robo pathway. Cell 107, 209–221.

Wu, J.Y., Feng, L., Park, H.T., Havlioglu, N., Wen, L., Tang, H., Bacon, K.B., Jiang, Z., Zhang, X., Rao, Y., 2001. The neuronal repellent Slit inhibits leukocyte chemotaxis induced by chemotactic factors. Nature 410, 948–952.

Xu, J., Wang, F., Van Keymeulen, A., Herzmark, P., Straight, A., Kelly, K., Takuwa, Y., Sugimoto, N., Mitchison, T., Bourne, H.R., 2003. Divergent signals and cytoskeletal assemblies regulate self-organizing polarity in neutrophils. Cell 114, 201–214.

Xu, Z., Jiang, J., Ford, G., Ford, B.D., 2004. Neuregulin-1 is neuroprotective and attenuates inflammatory responses induced by ischemic stroke. Biochem. Biophys. Res. Commun. 322, 440–446.

Yoshida, M., Westlin, W.F., Wang, N., Ingber, D.E., Rosenzweig, A., Resnick, N., Gimbrone Jr., M.A., 1996. Leukocyte adhesion to vascular endothelium induces E-selectin linkage to the actin cytoskeleton. J. Cell Biol. 133, 445–455.

Zhang, R.L., Chopp, M., Chen, H., Garcia, J.H., 1994a. Temporal profile of ischemic tissue damage, neutrophil response, and vascular plugging following permanent and transient (2H) middle cerebral artery occlusion in the rat. J. Neurol. Sci. 125, 3–10.

Zhang, R.L., Chopp, M., Li, Y., Zaloga, C., Jiang, N., Jones, M.L., Miyasaka, M., Ward, P.A., 1994b. Anti-ICAM-1 antibody reduces ischemic cell damage after transient middle cerebral artery occlusion in the rat. Neurology 44, 1747–1751.

Zheng, Z., Yenari, M.A., 2004. Post-ischemic inflammation: molecular mechanisms and therapeutic implications. Neurol. Res. 26, 884–892.

Zhu, Y., Saito, K., Murakami, Y., Asano, M., Iwakura, Y., Seishima, M., 2006. Early increase in mRNA levels of pro-inflammatory cytokines and their interactions in the mouse hippocampus after transient global ischemia. Neurosci. Lett. 393, 122–126.